Influence of Under-layer morphology on Structural and Magnetic Properties of Sputtered $Co_{81}Pd_{19}$ Films

Pairin Ponchaiya and Watcharee Rattanasakulthong*

Department of Physics, Faculty of Science, Kasetsart University, Bangkok, 10900, Thailand

*fsciwrr@ku.ac.th

Abstract. Sputtered $Co_{81}Pd_{19}$ films with thickness of about 60 nm were deposited on various under-layers (Co, Ni, Cr and Al) and on glass substrate. Structural, morphological and magnetic properties of $Co_{81}Pd_{19}$ films were investigated. All of prepared $Co_{81}Pd_{19}$ film showed CoPd-FCC phase in (111) direction on CoO-FCC (111), NiO-FCC (200), Cr-BCC (200) and (201) and AlO-FCC (200) phases of Co, Ni, Cr and Al under-layer, respectively. AFM images revealed that the film on Cr under-layers and glass substrate exhibited the maximum roughness with the highest grain size and the minimum roughness with the continuous grain size, respectively. Both parallel and perpendicular maximum coercive field were found in the film on glass under-layer and the film on Co-under-layer film showed the highest saturation magnetization from both in-plane and out-of-plane measurements. These results confirmed that the structural and magnetic properties of sputtered $Co_{81}Pd_{19}$ films were affected by under-layer surface roughness and morphology by the virtue of particle size and distribution on the under-layer film surface.

1. Introduction

Because of the perpendicular magnetic anisotropy, the large Kerr rotation and large negative magneto-striction at room temperature and high potential in application for magneto-optical recording, the CoPd thin film have been investigated by many researchers [1-6]. This alloyed film was fabricated in multi-layer [1-2] and granular [3-5] films by thermal evaporation [1], evaporation [2], electro-deposition [3], RF-magnetron sputtering [4] and molecular beam epitaxy [5]. Recently, the magneto-electric effect in CoPd thin film was investigated by first-principle calculation to study the effect of an external electrical field on surface atoms of the film [6]. In this research work, an effect of under-layer and substrate on structure, surface morphology and magnetic properties of $Co_{81}Pd_{19}$ films on different under-layers prepared by RF-magnetron sputtering was systematically studied.

2. Experiment

$Co_{81}Pd_{19}$ film was prepared on Co, Ni, Cr, and Al under-layers by RF-sputtering technique. The Co, Ni, Cr and Al under-layers were growth on glass substrate. The base pressure was lower than 1×10^{-5} mbar and the argon pressure during the sputtering process was about 1×10^{-3} mbar. The phase structure of prepared films was identified by X-ray diffractometor (XRD) with energy source using the CuK_{α} radiation. The thickness and chemical compositions of the sputtered films were determined by scanning electron microscope and energy dispersive spectrometer (EDS), respectively. The surface morphology and electrical resistance were analyzed by Atomic force microscopy (AFM) and 4-point

technique, respectively. The magnetic hysteresis loop of the film was investigated at room temperature in both parallel and perpendicular configurations by vibrating sample magnetometer (VSM).

3. Result and discussion

All sputtered $Co_{81}Pd_{19}$ films were stable and well adherent to the glass substrate and under-layers with smooth interfacing area between films and under-layers.

Cross-sectional SEM images show that average thickness of sputtered $Co_{81}Pd_{19}$ film was about 60 nm and those of Co, Ni, Cr and Al under-layers were 74, 105, 122 and 117 nm, respectively. The SEM and EDS results implied that the film thickness and chemical composition were a little varied on different under-layers. It may be due to the different lattice size of each under-layers and atom diffusion between film and under-layer.

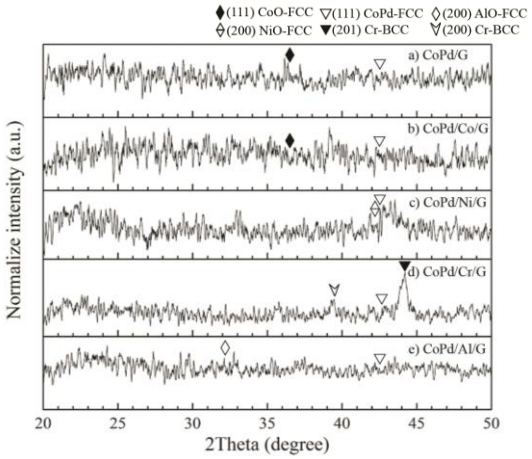

Figure 1. XRD patterns of $Co_{81}Pd_{19}$ film on a) glass substrate, b) Co, c) Ni, d) Cr and e) Al under-layers.

XRD patterns of $Co_{81}Pd_{19}$ film on glass substrate, Co, Ni, Cr and Al under-layers are shown in **Figure 1**. From XRD results, the $Co_{81}Pd_{19}$ film showed CoPd-FCC phase in (111) direction on CoO-FCC (111), NiO-FCC (200), Cr-BCC (200) and (201) and AlO-FCC (200) phases of Co, Ni, Cr and Al under-layer, respectively. Some amorphous phase was occurred in the film deposited on Ni and Cr under-layers. These results confirm that the films prefer orientating along the (111) direction in FCC structure of CoPd phase. A weak intensity of diffraction peaks was observed because the film thickness was very thin. The composition of the film was also confirmed by the EDS pattern and the magnetic properties. An amorphous phase of the film was slightly observed on Co, Ni and Al under-layers indicating the effect of the under-layer structure on the deposited film structure.

AFM images in **Figure 2** revealed the surface morphology of the $Co_{81}Pd_{19}$ and under-layer films over a scan area of 1 μm^2. Surface morphology of $Co_{81}Pd_{19}$ film was strongly dependent on under-layer surface morphology. $Co_{81}Pd_{19}$ film on glass substrate and on Co under-layer showed continuous grain whereas the film on Ni, Cr and Al under-layer displayed the columnar grain structure with different sizes and distributions. A medium size of columnar structure with the narrowest size distribution of the film surface was observed on Ni under-layer in Fig. 2 c) and a rather bigger columnar size with broader size distribution was founded on Cr under-layer in Fig. 2 d). The smaller columnar size with the broadest size distribution was established on Al under-layer in Fig 2. e). Comparing with native under-layer films, it implied that the fine gain size and regular distribution of Ni under-layer gave rise to the regular grain size and distribution of the film surface. These results implied that the smaller grain under-layer film generated a bigger grain film while a bigger grain under-layer created a smaller grain film. It can be concluded that under-layer surface morphology profoundly affected the $Co_{81}Pd_{19}$ film-surface characteristics.

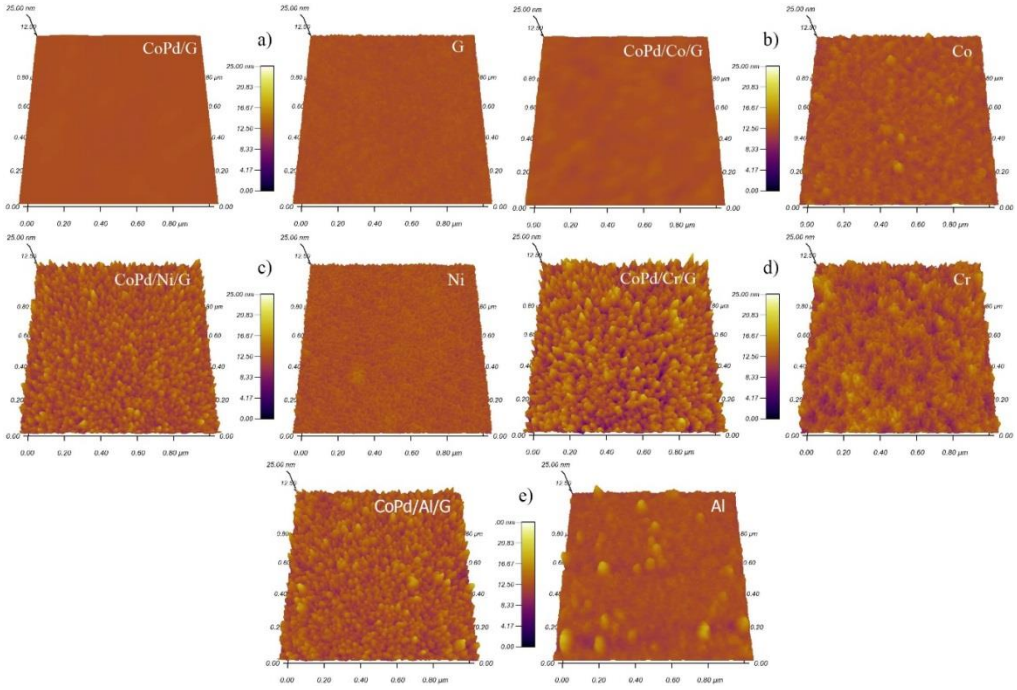

Figure 2. 3D-AFM images of $Co_{81}Pd_{19}$ film (Left) on a) glass substrate b) Co c) Ni d) Cr and e) Al under-layer (Right) over 1x1μm^2-area.

Surface roughness values over a scan area of 1 μm^2 and 25 μm^2 of the $Co_{81}Pd_{19}$ film on different under-layers were plotted as in **Figure 3**. The roughness of the film were 0.11 - 2.04 nm and 0.26-1.82 nm over an area of 1 μm^2 and 25 μm^2, respectively. The under-layer exhibited surface roughness between 0.29 nm to 1.64 over an area of 25 μm^2. The film on Cr under-layer showed the highest roughness of about 1.82 nm whereas the film on glass displayed the lowest surface roughness of 0.26 nm. It can be described that the Cr-BCC in (200) and (201) planes contributed the highest roughness whereas amorphous phase of glass supported the lowest roughness of the film. Modest roughness of 0.28 and 0.56 nm over an area of 1 μm^2 and 25 μm^2, respectively was observed on Co under-layer. It implied that matching direction of plane structure between film and under-layer gave rise to the lower roughness of the deposited film.

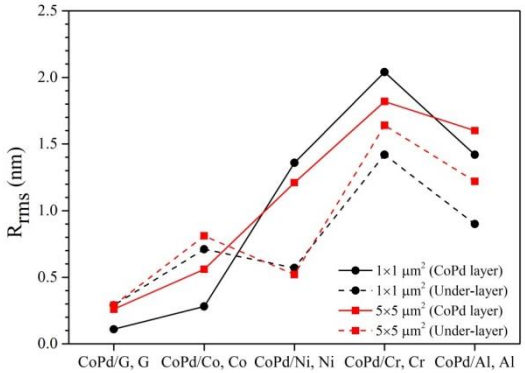

Figure 3. Surface roughness of the $Co_{81}Pd_{19}$ film on glass substrate and under-layers over scan area of 1x1μm^2 and 5x5μm^2.

Magnetic properties sputtered films on different under-layers in perpendicular and parallel configurations at room temperature were showed in **Figure 4**. The film on various under-layers exhibited the ferromagnetic phase under an applied magnetic field of 10 kG. Perpendicular hysteresis loop reached saturation whereas parallel hysteresis loop displayed unsaturation under magnetic field of 10 kG. These results implied that all $Co_{81}Pd_{19}$ films on various under-layers showed the perpendicular magnetic anisotropy excluding the film on the Ni under-layer. Both parallel and perpendicular maximum coercive fields were found in the film on glass substrate and the film on Co-under-layer film showed the highest saturation magnetization. The highest saturation was contributed from the highest magnetic phase of Co concentration. **Figure 5** displayed the magnetic parameters of the film on different under-layers. It can be described that the continuous grain size with the lowest surface roughness of the $Co_{81}Pd_{19}$ film promoted the perpendicular anisotropy and the amorphous phase of glass substrate not only supported the existence of a very fine grain size and the lowest surface roughness but also induced a perpendicular magnetic anisotropy.

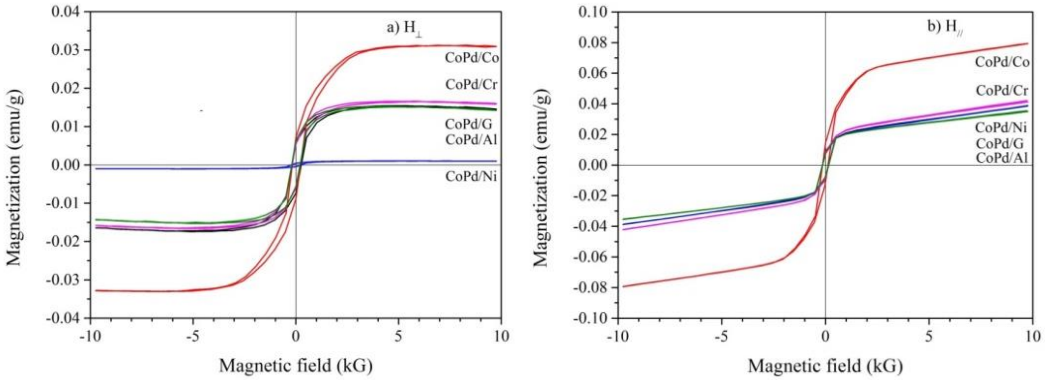

Figure 4. VSM results of the $Co_{81}Pd_{19}$ film when an applied magnetic field was (a) perpendicular and (b) parallel to the film plane.

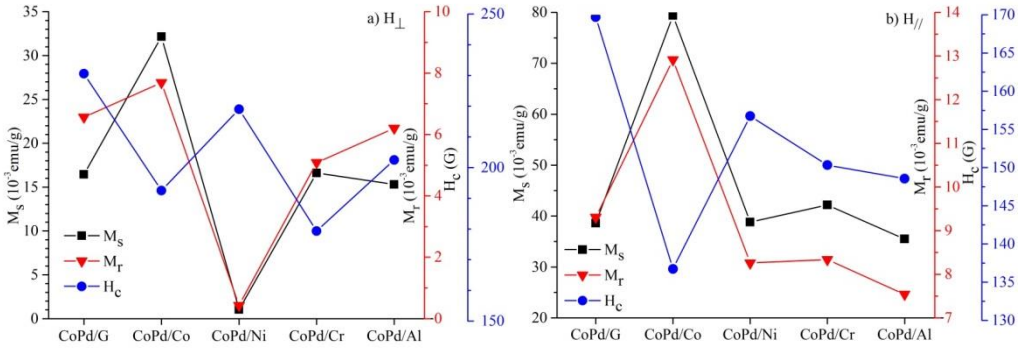

Figure 5. Magnetic parameters of the $Co_{81}Pd_{19}$ film when an applied magnetic field was (a) perpendicular and (b) parallel to the film plane.

4. Conclusions

Sputtered $Co_{81}Pd_{19}$ films presented the CoPd-FCC phase in (111) direction on CoO-FCC (111), NiO-FCC (200), Cr-BCC (200) and (201) and AlO-FCC (200) phases of Co, Ni, Cr and Al under-layer, respectively. The film on Cr under-layers exhibited the maximum roughness with the highest grain size and that on glass substrate showed the minimum roughness with the continuous grain size. All films showed ferromagnetic phase at room temperature and the film on glass substrate had maximum parallel and perpendicular maximum coercive fields. It can be concluded that the structure surface morphology and magnetic properties of the $Co_{81}Pd_{19}$ film were affected by surface roughness

of the under-layer and substrate, and the morphology by virtue of structure phase, grain size and distribution of the under-layer and substrate. The amorphous phase with a very fine grain size and the lowest surface roughness of glass substrate significantly induced a perpendicular magnetic anisotropy.

References

[1] den Broeder F J A, Donkersloot H C, Draaisma H J G, and de Jonge W J M 1987 *J Appl Phys* **61** 4317

[2] Li Bihan, Liu Xinming, Zhu Mei, Wang Zongbin, Adeyeye A O and Choi W K 2015 *J Nanosci Nanotechnol* **15** 4332

[3] Takata F M and Sumodjo P T A 2007 *Electrochimica Acta* **52** 6089

[4] Yabuhara Osamu, Ohtake Mitsuru, Tobari Kouske, Nishiyama Tsutomu, Kirino Fumiyoshi and Futamoto Masaaki 2011 *Thin Solid Films* **519** 8359

[5] Morgan Caitlin, Schmalbuch Klaus, Schmalbuch Felipe, Schmalbuch Claus M and Meyer Carola 2013 *J Magn Magn Mater* **325** 112

[6] Manchanda P, Skomski R, Solanki A K, Kumar P S A and Kashyap A 2011 *IEEE Trans Magn* **47** 4391

Acknowledgements

This research is financially supported by The Graduate School, Kasetsart University. The matching fund by Department of Physics and Faculty of Science, Kasetsart University are also acknowledged.